

1     **A GENERALISED RANDOM ENCOUNTER MODEL FOR ESTIMATING**  
2                   **ANIMAL DENSITY WITH REMOTE SENSOR DATA**

3     **Running title: A generalised random encounter model for animals.**

4     **Word count:**

5     **Authors:**

6     Tim C.D. Lucas<sup>1,2,3</sup>, Elizabeth A. Moorcroft<sup>1,4,5</sup>, Robin Freeman<sup>5</sup>, Marcus J. Rowcliffe<sup>5</sup>,  
7     Kate E. Jones<sup>2,5</sup>

8     **Addresses:**

9     1 CoMPLEX, University College London, Physics Building, Gower Street, Lon-  
10    don, WC1E 6BT, UK

11    2 Centre for Biodiversity and Environment Research, Department of Genetics,  
12    Evolution and Environment, University College London, Gower Street, London,  
13    WC1E 6BT, UK

14    3 Department of Statistical Science, University College London, Gower Street,  
15    London, WC1E 6BT, UK

16    4 Department of Computer Science, University College London, Gower Street,  
17    London, WC1E 6BT, UK

18    5 Institute of Zoology, Zoological Society of London, Regents Park, London, NW1  
19    4RY, UK

20    **Corresponding authors:**

21    Kate E. Jones,  
22    Centre for Biodiversity and Environment Research,  
23    Department of Genetics, Evolution and Environment,  
24    University College London,  
25    Gower Street,  
26    London,  
27    WC1E 6BT,  
28    UK

1 kate.e.jones@ucl.ac.uk

2

3 Marcus J. Rowcliffe,  
4 Institute of Zoology,  
5 Zoological Society of London,  
6 Regents Park,  
7 London,  
8 NW1 4RY,  
9 UK  
10 marcus.rowcliffe@ioz.ac.uk

## 1. ABSTRACT

**1:** Wildlife monitoring technology has advanced rapidly and the use of remote sensors such as camera traps, and acoustic detectors is becoming common in both the terrestrial and marine environments. Current capture-recapture or distance methods to estimate abundance or density require individual recognition of animals or knowing the distance of the animal from the sensor, which is often difficult. A method without these requirements, the random encounter model (REM), has been successfully applied to estimate animal densities from count data generated from camera traps. However, count data from acoustic detectors do not fit the assumptions of the REM due to the directionality of animal signals.

**2:** We developed a generalised REM (gREM), to estimate absolute animal density from count data from both camera traps and acoustic detectors. We derived the gREM for different combinations of sensor detection widths and animal signal widths (a measure of directionality). We tested the accuracy and precision of this model using simulations of different combinations of sensor detection widths and animal signal widths, number of captures, and models of animal movement.

**3:** We find that the gREM produces accurate estimates of absolute animal density for all combinations of sensor detection widths and animal signal widths. However, larger sensor detection and animal signal widths were found to be more precise. While the model is accurate for all capture efforts tested, the precision of the estimate increases with the number of captures. We found no effect of different animal movement models tested on the accuracy and precision of the gREM.

**4:** We conclude that the gREM provides an effective method to estimate absolute animal densities from remote sensor count data over a range of sensor and animal signal widths. The gREM is applicable for use for count data obtained in both marine and terrestrial environments, visually or acoustically (e.g., big cats, sharks, birds, bats and cetaceans). As sensors such as camera traps and acoustic detectors become more ubiquitous, the gREM will be increasingly useful for monitoring animal populations across broad spatial, temporal and taxonomic scales.

1 1.1. **Keywords.** Acoustic detection, Camera traps, Marine, Population monitor-  
2 ing, Simulations, Terrestrial

## 3 2. INTRODUCTION

4 Wildlife monitoring important (declines in populations, global declines) Wildlife  
5 monitoring tech growing in sophistication and widespread (remote sensors visual  
6 and acoustic) Difficult to estimate abundance and densities (needed for monitor-  
7 ing) Current methods are often inadequate because of specific data requirements  
8 (marked individuals) REM developed for camera trap data, doesn't need these as-  
9 sumptions but has limitations Specifically sensor widths - different environments  
10 might need more flexibility (examples) and signal directionality assumptions (ex-  
11 amples) - method has been optimised for terrestrial large animals acoustic moni-  
12 toring becoming more common method of monitoring but has additional sensor  
13 width problems (examples) and directionality of signals (examples). Currently  
14 the count data from acoustic monitoring is used for monitoring in different ways  
15 (examples). Another limitation to using these sensors is lack of guidelines on how  
16 survey effort impacts the accuracy and precision of estimates (guidelines would be  
17 useful. practically can only be done within simulated environment, rarely done)  
18 We develop gREM and tested it and come up with specific recommendations for  
19 its use (providing code for implementation). we controlled for different animal  
20 movement by testing the robustness of gREM with different movement model (ex-  
21 amples).

22 Animal population size is one of the fundamental measures needed in ecology  
23 and conservation. The absolute size of a population has important implications for  
24 a range of issues such as genetic diversity (O'Brien *et al.*, 1985; Fischer *et al.*, 2000;  
25 Willi *et al.*, 2005), sensitivity to stochastic fluctuations (Richter-Dyn & Goel, 1972;  
26 Wright & Hubbell, 1983) and risk of extinction (Purvis *et al.*, 2000). Sensor technol-  
27 ogy, such as camera traps (Rowcliffe & Carbone, 2008; Ahumada *et al.*, 2011) and  
28 acoustic detectors (O'Farrell & Gannon, 1999; Mellinger & Stafford, 2007; Jones  
29 *et al.*, 2011) are becoming increasingly used to survey animal populations, as they  
30 are efficient, relatively cheap and non-invasive (Gese, 2001; O'Brien *et al.*, 2003;  
31 Silveira *et al.*, 2003), allowing for surveys over large areas and long periods.



1  $\theta$  less than  $\pi$  radians and detection distance  $r$  (Appendix S1 for a list of sym-  
 2 bols), giving a circular sector within which animals can be captured (detection  
 3 zone)(Figure ??). However, in order to apply this approach more generally, and  
 4 in particular to acoustic detectors, we need both to relax the constraint on sen-  
 5 sor detection width, and allow for animals with directional signals. We therefore  
 6 model the animal as having an associated signal width  $\alpha$ . We derive models for  
 7 any detection width,  $\theta$ , between 0 and  $2\pi$  and any signal width,  $\alpha$ , between 0 and  
 8  $2\pi$ , starting with the simplest model, the gas model (where  $\theta = 2\pi$  and  $\alpha = 2\pi$ ).

9 3.1.1. *Gas Model*. Here we derive the gas model where sensors can capture ani-  
 10 mals in any direction and animals give out signals in all directions ( $\theta = 2\pi$  and  
 11  $\alpha = 2\pi$ ). We assume that animals are in a homogeneous environment, and move  
 12 in straight lines of random direction with velocity  $v$ . We allow that our stationary  
 13 sensor can capture animals at a detection distance  $r$  and that if an animal moves  
 14 within this detection zone they are captured with a probability of one, while ani-  
 15 mals outside the region are never captured.

16 For computational simplicity in later models, we then consider relative velocity  
 17 from the reference frame of the animals. Conceptually, this requires us to imagine  
 18 that all animals are stationary and randomly distributed in space, while the sensor  
 19 moves with velocity  $v$ . If we calculate the area covered by the sensor during the  
 20 survey period we can estimate the number of animals it should capture. As a circle  
 21 moving across a plane, the area covered by the sensor per unit time is  $2rv$ . The  
 22 number of expected captures,  $z$ , for a survey period of  $t$ , with an animal density of  
 23  $D$  is  $z = 2rvtD$ . To estimate the density, we rearrange to get  $D = z/2rvt$ .

24 3.1.2. *Discontinuity in detector and signal width combinations*. Although  $\theta$  and  $\alpha$  vary  
 25 continuously, we find that there are many discontinuities in the derivation of the  
 26 model depending on their combination. For different values of  $\theta$  and  $\alpha$ , the area  
 27 covered per unit time is no longer given by  $2rv$ . Instead of the sensor having a  
 28 diameter of  $2r$ , the sensor has a diameter (the profile  $p$ ) that changes with approach  
 29 angle of the sensor and the animal. Thus  $p$  is the value of the diameter of the  
 30 sensor averaged across all possible approach angles. However, there is not one  
 31 equation to calculate  $p$  for every combination of  $\theta$  and  $\alpha$ . Instead, different areas of

1 parameter space have different equations to calculate profiles. Therefore we have  
 2 identified the combinations of  $\theta$  and  $\alpha$  for which the equation is the same, and  
 3 derive  $p$  for each combination (Figure ??). We have derive one model SE2 as an  
 4 example (where  $4\pi - 2\alpha < \theta < 2\pi$ ,  $0 < \alpha < \pi$ ) and the remaining derivations are  
 5 included in Appendix S2.

6 Many of these models have the same functional form, and are therefore grouped  
 7 together as can be seen in Figure 3, all of the sub models can be seen in Figure 1 in  
 8 Appendix S1. The upper right corner of Figure 3 being the gas model as derived  
 9 above and 'REM' is the model from (Rowcliffe *et al.*, 2008).

10 When the detection angle is smaller than  $\pi$  we need to explicitly write functions  
 11 for the width of the profile for every approach angle. We then use these functions  
 12 to find the average profile for all approach angles by integrating across all  $2\pi$  an-  
 13 gles of approach and dividing by  $2\pi$ . In practice, as the models are all left/right  
 14 symmetrical we can integrate across  $\pi$  angles of approach and divide by  $\pi$ .

15 3.1.3. *Example derivation.* To work through one example that contains both  $\theta$  and  
 16  $\alpha$  we will examine model SE2. All other derivations are described in Appendix S1  
 17 with computer algebra scripts in Appendix S2, and the R script of the implemented  
 18 models in Appendix S3.

19 The focal angle is denoted by  $x_i$  and is the angle which we integrate over. The  
 20 subscript  $i$  distinguishes different approach angles. For model SE2 we examine  $x_1$   
 21 with  $x_1 = \pi/2$  being an approach angle directly towards the sensor (Figure 1).

22 By rotating anticlockwise, from  $x_1 = \pi/2$  the detection zone is  $2r$  wide, as shown  
 23 by the red line in Figure 1. However, an animal will only be detected if it ap-  
 24 proaches the detector so that as it enters the detection region the angle between  
 25 the direction of approach and the direction towards the sensor is less than  $\alpha/2$ .  
 26 The width of the profile within which the animal will be detected is therefore  
 27  $2r \sin(\alpha/2)$ . At  $x_1 = \theta/2 + \pi/2 - \alpha/2$  we reach a point where the right hand side  
 28 of the profile (relative to the approach direction) is not limited by the call angle  
 29 but is limited by the detection angle instead. From here the profile width is there-  
 30 fore  $r \sin(\alpha/2) + r \cos(x_1 - \theta/2)$ . Finally, at  $x_1 = 5\pi/2 - \theta/2 - \alpha/2$  an animal can again  
 31 be detected from the right side of the detector; the approach angle is far enough

round to see past the ‘blind spot’ of the sensor. In this region, until  $x_1 = 3\pi/2$ , the width of the profile is again  $2r \sin(\alpha/2)$ . We have therefore characterised the profile width for  $\pi$  radians of rotation (from directly towards the sensor to directly behind the sensor). To find the average profile width for any angle of approach, we integrate these functions over their appropriate intervals of  $x_1$  and divide by  $\pi$  to give:

$$p = \frac{1}{\pi} \left( \int_{\frac{\pi}{2}}^{\frac{\pi}{2} + \frac{\theta}{2} - \frac{\alpha}{2}} 2r \sin\left(\frac{\alpha}{2}\right) dx_1 + \int_{\frac{\pi}{2} + \frac{\theta}{2} - \frac{\alpha}{2}}^{\frac{5\pi}{2} - \frac{\theta}{2} - \frac{\alpha}{2}} r \sin\left(\frac{\alpha}{2}\right) + r \cos\left(x_1 - \frac{\theta}{2}\right) dx_1 + \int_{\frac{5\pi}{2} - \frac{\theta}{2} - \frac{\alpha}{2}}^{\frac{3\pi}{2}} 2r \sin\left(\frac{\alpha}{2}\right) dx_1 \right)$$

$$= \frac{r}{\pi} \left( \theta \sin\left(\frac{\alpha}{2}\right) - \cos\left(\frac{\alpha}{2}\right) + \cos\left(\frac{\alpha}{2} + \theta\right) \right) \quad \text{eqn 1}$$

Then, as with the gas model, this term is used to calculate density

$$D = z/vtp \quad \text{eqn 2}$$

We can also see what causes this model to be discontinuously different to SE3. Examine the profile at  $x_1 = \theta/2 + \pi/2$  (the profile is perpendicular to the edge of the blind spot.) We see that there is potentially a case where the left side of the profile is  $r \sin(\alpha/2)$  while the right side is zero. This profile does not exist if we return to the full  $2r \sin(\alpha/2)$  profile before  $x_1 = \theta/2 + \pi/2$ . Therefore we solve  $5\pi/2 - \theta/2 - \alpha/2 < \theta/2 + \pi/2$ . We find that this new profile only exists if  $\alpha < 4\pi - 2\theta$ . This inequality defines the line separating models SE2 and its neighbouring model, SE3.

While specifying the models had to be done by hand, the calculation of the solutions was done using SymPy (SymPy Development Team, 2014) in Python. The models were checked for errors with a number of tests. The models were checked against each other by checking that models which are adjacent in parameter space are equal at the boundary between them (e.g. eqn 1 is equal to  $2r$  as in the gas model when  $\alpha = \pi$  and  $\theta = 2\pi$ ). Models that border  $\alpha = 0$  should have  $p = 0$  when  $\alpha = 0$  and this was checked for (e.g. eqn 1 is zero when  $\alpha = 0$  and  $\theta = 2\pi$ ). We checked that all solutions are between 0 and  $2r$  and that each integral, divided by the range of angles that it is integrated over is between 0 and  $2r$ . These tests are included in Appendix S2.



1 **3.2. Simulation Model.** In order to validate the gREM we developed a spatially  
 2 explicit simulation of animal movement. By simulating animal movement with  
 3 various movement patterns within a continuous space containing sensors we cal-  
 4 culated how many animal contacts the sensors would have detected.

5 Each simulation consisted of a 7.5 km by 7.5 km square (with periodic bound-  
 6 aries) and was populated with a density of 70 animals  $\text{km}^{-2}$  to match an expected  
 7 maximum density of mammals in the wild (Damuth, 1981), creating a total of 3937  
 8 animals per simulation which were placed randomly at the start of the simulation.  
 9 Animal movement was simulated with a simple movement model, characterised  
 10 by a random movement distance for each discrete time step, at the end of each step  
 11 the animal could change direction with a uniform distribution up to a maximum  
 12 specified angle. The simulation lasted for  $N$  steps of duration  $T$  during which the  
 13 animals moved with an average speed,  $v$ . The distance travelled in each time step,  
 14  $d$ , was sampled from a Normal distribution with mean distance,  $\mu_d = vT$ , and  
 15 standard deviation  $\sigma_d = vT/10$ . An average speed,  $v = 40 \text{ km days}^{-1}$ , was cho-  
 16 sen as this represents the largest day range of terrestrial animals (Carbone *et al.*,  
 17 2005), and represents the upper limit of realistic speeds. To reduce computation  
 18 effort, a single set of 100 simulations was run for a long duration which could be  
 19 subsampled.

20 Animals were counted as they moved in and out of the detection zone of sta-  
 21 tionary detectors in the simulation. Multiple detectors were set up in each simula-  
 22 tion with varying detection angles with the results recorded separately. The details  
 23 of each individual capture event, including the angle between the animals head-  
 24 ing and the sensor, were saved from this information the number of capture events  
 25 can be calculated for a given call angle. The total number of these detections were  
 26 summed for each set of parameters in the simulation, the gREM was then applied  
 27 in order to estimate the density in the simulation. The difference between the true  
 28 input density and density estimated by the gREM were used to evaluate the bias  
 29 in the analytical models. If the gREM is correct the mean difference between the  
 30 two values were expected to converge to zero as sample size increases. For each  
 31 of the 100 simulations we calculate the error (the difference between the known

1 and estimated density) and so we got a distribution of errors which was approxi-  
 2 mately normal. We constructed boxplots of the estimates error to graphically test  
 3 for significant differences between the true and estimated densities.

4 All the derived models were tested to demonstrate the accuracy and precision  
 5 of the gREM while the assumptions of the analytical models were met. We selected  
 6 four example models (models NW1, SW1, NE1, and SE3, where these names refer  
 7 to Figure 1 in Appendix S1) for demonstrating the accuracy and precision of the  
 8 gREM with low captures rates, and the accuracy and precision when movement  
 9 patterns brake the assumptions of the gREM. We specifically looked at a non-  
 10 continuous movement, and a range of correlated random walks, both of which  
 11 would be seen in real field conditions. The four models were chosen as they rep-  
 12 resent one model from each quadrant of Figure 3. The accuracy and precision of  
 13 all the derived models in the gREM follow the same pattern as the four that have  
 14 been shown in the main text.

## 15 4. RESULTS

16 **4.1. Analytical model.** Model results have been derived for each zone with all  
 17 models except the gas model and REM being newly derived here. However, many  
 18 models, although derived separately, have the same expression for  $p$ . Figure 3  
 19 shows the expression for  $p$  in each case. The general equation for density, using  
 20 the correct expression for  $p$  is then substituted into eqn 2.

21 Although more thorough checks are performed in Appendix S3, it can be seen  
 22 that all adjacent expressions in Figure 3 are equal when expressions for the bound-  
 23 aries between them are substituted in.

24 **4.2. Simulation model.** For each model we compared the estimated densities to  
 25 the true densities in a simulation. None of the models showed any evidence of any  
 26 significant differences between the estimated and true density values (Figure 4).  
 27 The precision of the models do vary however. The standard deviation of the error  
 28 is strongly related to the call and sensor width (Figure 5), such that larger widths  
 29 have greater precision. However, even the models with small call and sensor an-  
 30 gles have a relatively high level of precision.

1 The precision of the model is dependent on the number of captures during the  
 2 survey. In Figure 7 we can see that the model precision gets greater as the num-  
 3 ber of captures increase. As the number of captures reaches about 100 then the  
 4 coefficient of variation falls below 10% which could be considered negligible.

#### 5 4.2.1. *Use of the gREM when animal movement is not consistent with model assumptions.*

6 Simulating start-stop instead of continuous movement had no effect the accuracy,  
 7 or the precision, of the estimates (Figure 9) as long as the true overall speed of the  
 8 animal is known. Relaxing straight line movement to allow random or correlated  
 9 random walks did not effect the accuracy of the method (Figure 11). We allowed  
 10 animals to change direction up to a maximum value at the end of each step, picked  
 11 from a uniform distribution where the maximum angle ranged from 0 to  $\pi$ , which  
 12 corresponds to straight line movement and random walk respectively. There is  
 13 no significant difference in the variance for the change, this could be because of  
 14 the between the step length of the animal movement, 15 minutes, means that im-  
 15 mediate double counting of the same animal is unlikely. In the case where large  
 16 directional changes are likely to occur within short periods of time leading to dou-  
 17 ble counting of the same animal within a short period of time may need to be  
 18 adjusted because of this.

## 19 5. DISCUSSION

20 We have developed the gREM such that it can be used to estimate density from  
 21 acoustic and optical sensors. This has entailed a generalisation of the gas model  
 22 and the model in (Rowcliffe *et al.*, 2008) to be applicable to any combination of  
 23 sensor width and call directionality. We have used simulations to show, as a proof  
 24 of principle, that these models are accurate and precise.

25 The gREM is therefore available for the estimation of density of a number of  
 26 taxa of importance to conservation, zoonotic diseases and ecosystem services. The  
 27 models provided are suitable for certain groups for which there are currently no,  
 28 or few, effective methods for density estimation. Any species that would be consis-  
 29 tently recorded at least once when within range of a detector would be a suitable  
 30 subject for the gREM, such as bats (Kunz *et al.*, 2009), songbirds (Buckland & Han-  
 31 del, 2006), Cetaceans (Marques *et al.*, 2009) or forest primates (Hassel-Finnegan

1 *et al.*, 2008). Within increasing technological capabilities, this list of species is likely  
2 to increase dramatically.

3 Importantly the methods are noninvasive and do not require human marking or  
4 naturally identifying marks (as required for mark-recapture models). This makes  
5 them suitable for large, continuous monitoring projects with limited human re-  
6 sources. It also makes them suitable for species that are under pressure, species  
7 that cannot naturally be individually recognised or species that are difficult or  
8 dangerous to catch.

9 From our simulations we believe that this method has the potential produce  
10 accurate and precise estimates for many different species, using either camera or  
11 acoustic detectors. When choosing detectors a researcher should pick the detector  
12 with the largest radius and detection angle possible, but whilst a small capture  
13 area may reduce precision there is only a limited impact on the overall precision  
14 of the model (Figure 5). A range of factors will affect the overall precision of the  
15 model, like size of detection zone, speed of animal, density of animals and length  
16 of survey which are reflected in the number of captures. Increasing the number of  
17 captures leads to more precise estimates, for species which more slower, or have  
18 occur at lower densities, then the detection zone and length of survey need to be  
19 increased to compensate so that at least 100 captures are collected (Figure 7).

20 Within the simulation we have assumed an equal density across the entire world,  
21 however in a field environment the situation would be much more complex, with  
22 additional variation coming from local changes in density between camera sites.  
23 We also assume perfect knowledge of the average speed of an animal and size of  
24 the detection zone, and instant triggering of the camera. All of which may lead to  
25 possible bias or decreased precision.

26 Although we have used simulations to validate these models, much more ro-  
27 bust testing is needed. Although difficult, proper field test validation would be  
28 required before the models could be fully trusted. Note, however, that the REM  
29 (Rowcliffe *et al.*, 2008) has been field tested. Both Rowcliffe *et al.* (2008) and Zero  
30 *et al.* (2013) both found that the REM were effective manner of estimating animal  
31 densities (Rowcliffe *et al.*, 2008; Zero *et al.*, 2013). There was some discrepancies  
32 between the REM and the census methodologies found by Rovero and Marshall

1 which may have been down to lack of knowledge of wild animal speed, and an  
2 underestimate in census results (Rovero & Marshall, 2009). In some taxa gold stan-  
3 dard methods of estimating animal density exist, such as capture mark recapture.  
4 Where these gold standard exist, and have been proved to work, a simultaneous  
5 gREM study could be completed to test the accuracy under field conditions. An  
6 easier way to continue to evaluate the models is to run more extensive simulations  
7 which break the assumptions of the analytical models. The main element that  
8 cannot be analytically treated is the complex movement of real animals. There-  
9 fore testing these methods against true animal traces, or more complex movement  
10 models would be useful.

11 There are a number of positive extensions to the gREM which could be devel-  
12 oped in the future. The original gas model was formulated for the case where both  
13 subjects, either animal and detector, or animal and animal, are moving (Hutchin-  
14 son & Waser, 2007). Indeed any of the models with animals that are equally de-  
15 tectable in all directions ( $\alpha = 2\pi$ ) can be trivially expanded for moving by sub-  
16 stituting the sum of the average animal velocity and the sensor velocity for  $v$  as  
17 used here. However, when the animal has a directional call, the extension be-  
18 comes much less simple. The approach would be to calculate again the mean  
19 profile width. However, for each angle of approach, one would have to average  
20 the profile width for an animal facing in any direction (i.e. not necessarily moving  
21 towards the sensor) weighted by the relative velocity of that direction. There are  
22 a number of situations where a moving detector and animal could occur and as  
23 such may be advantage to have a method of estimating densities from the data  
24 collected, e.g. an acoustic detector based off a boat when studying Cetacea or sea  
25 birds (Yack *et al.*, 2013).

26 Another interesting, and so far unstudied problem, is edge effects caused by  
27 trigger delays (the delay between sensing an animal and attempting to record the  
28 encounter) and time expansion acoustic detectors which repeatedly turn on an off  
29 during sampling. Both of these have potential biases as animals can move through

1 the detection zone without being detected. The models herein are formulated as-  
2 suming constant surveillance and so the error quickly becomes negligible. For ex-  
3 ample, if it takes longer for the recording device to be switched on than the length  
4 of some animal calls there could be a systematic underestimation of density.

## 5 6. ACKNOWLEDGMENTS

## 6 REFERENCES

- 7 Ahumada, J.A., Silva, C.E., Gajapersad, K., Hallam, C., Hurtado, J., Martin, E.,  
8 McWilliam, A., Mugerwa, B., O'Brien, T., Rovero, F. *et al.* (2011) Community  
9 structure and diversity of tropical forest mammals: data from a global camera  
10 trap network. *Philosophical Transactions of the Royal Society B: Biological Sciences*,  
11 **366**, 2703–2711.
- 12 Barlow, J. & Taylor, B. (2005) Estimates of sperm whale abundance in the north-  
13 eastern temperate pacific from a combined acoustic and visual survey. *Marine*  
14 *Mammal Science*, **21**, 429–445.
- 15 Buckland, S.T. & Handel, C. (2006) Point-transect surveys for songbirds: robust  
16 methodologies. *The Auk*, **123**, 345–357.
- 17 Carbone, C., Cowlishaw, G., Isaac, N.J. & Rowcliffe, J.M. (2005) How far do ani-  
18 mals go? Determinants of day range in mammals. *The American Naturalist*, **165**,  
19 290–297.
- 20 Damuth, J. (1981) Population density and body size in mammals. *Nature*, **290**,  
21 699–700.
- 22 Fischer, M., Van Kleunen, M. & Schmid, B. (2000) Genetic allee effects on perfor-  
23 mance, plasticity and developmental stability in a clonal plant. *Ecology Letters*,  
24 **3**, 530–539.
- 25 Gese, E.M. (2001) Monitoring of terrestrial carnivore populations. *USDA National*  
26 *Wildlife Research Center-Staff Publications*, p. 576.
- 27 Hassel-Finnegan, H.M., Borries, C., Larney, E., Umponjan, M. & Koenig, A. (2008)  
28 How reliable are density estimates for diurnal primates? *International Journal of*  
29 *Primatology*, **29**, 1175–1187.

- 1 Hutchinson, J.M.C. & Waser, P.M. (2007) Use, misuse and extensions of “ideal gas”  
2 models of animal encounter. *Biological Reviews of the Cambridge Philosophical So-*  
3 *ciet*y, **82**, 335–359.
- 4 Jones, K.E., Russ, J.A., Bashta, A.T., Bilhari, Z., Catto, C., Csősz, I., Gorbachev,  
5 A., Győrfi, P., Hughes, A., Ivashkiv, I. *et al.* (2011) Indicator bats program: a  
6 system for the global acoustic monitoring of bats. *Biodiversity Monitoring and*  
7 *Conservation: Bridging the Gap between Global Commitment and Local Action*, pp.  
8 211–247.
- 9 Karanth, K. (1995) Estimating tiger (*Panthera tigris*) populations from camera-trap  
10 data using capture–recapture models. *Biological Conservation*, **71**, 333–338.
- 11 Kunz, T.H., Betke, M., Hristov, N.I. & Vonhof, M. (2009) Methods for assessing  
12 colony size, population size, and relative abundance of bats. *Ecological and be-*  
13 *havioral methods for the study of bats* (TH Kunz and S Parsons, eds) 2nd ed Johns  
14 Hopkins University Press, Baltimore, Maryland, pp. 133–157.
- 15 Marques, T.A., Munger, L., Thomas, L., Wiggins, S. & Hildebrand, J.A. (2011) Es-  
16 timating North Pacific right whale (*Eubalaena japonica*) density using passive  
17 acoustic cue counting. *Endangered Species Research*, **13**, 163–172.
- 18 Marques, T.A., Thomas, L., Ward, J., DiMarzio, N. & Tyack, P.L. (2009) Estimating  
19 cetacean population density using fixed passive acoustic sensors: An example  
20 with Blainville’s beaked whales. *The Journal of the Acoustical Society of America*,  
21 **125**, 1982–1994.
- 22 Mellinger, D. & Stafford, K. (2007) Fixed passive acoustic observation methods for  
23 Cetaceans. *Oceanography*, **20**, 36.
- 24 O’Brien, S., Roelke, M., Marker, L., Newman, A., Winkler, C., Meltzer, D., Colly,  
25 L., Evermann, J., Bush, M. & Wildt, D.E. (1985) Genetic basis for species vulner-  
26 ability in the cheetah. *Science*, **227**, 1428–1434.
- 27 O’Brien, T.G., Kinnaird, M.F. & Wibisono, H.T. (2003) Crouching tigers, hidden  
28 prey: Sumatran tiger and prey populations in a tropical forest landscape. *Animal*  
29 *Conservation*, **6**, 131–139.
- 30 O’Farrell, M.J. & Gannon, W.L. (1999) A comparison of acoustic versus capture  
31 techniques for the inventory of bats. *Journal of Mammalogy*, pp. 24–30.

- 1 Purvis, A., Gittleman, J.L., Cowlshaw, G. & Mace, G.M. (2000) Predicting extinction risk in declining species. *Proceedings of the Royal Society of London Series B: Biological Sciences*, **267**, 1947–1952.
- 4 Richter-Dyn, N. & Goel, N.S. (1972) On the extinction of a colonizing species. *Theoretical Population Biology*, **3**, 406–433.
- 6 Rovero, F. & Marshall, A.R. (2009) Camera trapping photographic rate as an index of density in forest ungulates. *Journal of Applied Ecology*, **46**, 1011–1017.
- 8 Rowcliffe, J.M. & Carbone, C. (2008) Surveys using camera traps: are we looking to a brighter future? *Animal Conservation*, **11**, 185–186.
- 10 Rowcliffe, J., Field, J., Turvey, S. & Carbone, C. (2008) Estimating animal density using camera traps without the need for individual recognition. *Journal of Applied Ecology*, **45**, 1228–1236.
- 13 Silveira, L., Jacomo, A.T. & Diniz-Filho, J.A.F. (2003) Camera trap, line transect census and track surveys: a comparative evaluation. *Biological Conservation*, **114**, 351–355.
- 16 Soisalo, M.K. & Cavalcanti, S. (2006) Estimating the density of a jaguar population in the Brazilian Pantanal using camera-traps and capture-recapture sampling in combination with GPS radio-telemetry. *Biological Conservation*, **129**, 487–496.
- 19 SymPy Development Team (2014) *SymPy: Python library for symbolic mathematics*.
- 20 Trolle, M. & Kéry, M. (2003) Estimation of ocelot density in the Pantanal using capture-recapture analysis of camera-trapping data. *Journal of mammalogy*, **84**, 607–614.
- 23 Trolle, M., Noss, A.J., Lima, E.D.S. & Dalponte, J.C. (2007) Camera-trap studies of maned wolf density in the Cerrado and the Pantanal of Brazil. *Biodiversity and Conservation*, **16**, 1197–1204.
- 26 Willi, Y., Van Buskirk, J. & Fischer, M. (2005) A threefold genetic allee effect population size affects cross-compatibility, inbreeding depression and drift load in the self-incompatible *Ranunculus reptans*. *Genetics*, **169**, 2255–2265.
- 29 Wright, S.J. & Hubbell, S.P. (1983) Stochastic extinction and reserve size: a focal species approach. *Oikos*, pp. 466–476.
- 31 Yack, T.M., Barlow, J., Calambokidis, J., Southall, B. & Coates, S. (2013) Passive acoustic monitoring using a towed hydrophone array results in identification of



- 1 a previously unknown beaked whale habitat. *The Journal of the Acoustical Society*  
2 *of America*, **134**, 2589–2595.
- 3 Yapp, W. (1956) The theory of line transects. *Bird study*, **3**, 93–104.
- 4 Zero, V.H., Sundaresan, S.R., O'Brien, T.G. & Kinnaird, M.F. (2013) Monitoring  
5 an endangered savannah ungulate, Grevy's zebra (*Equus grevyi*): choosing a  
6 method for estimating population densities. *Oryx*, **47**, 410–419.

Symbol	Description	Units
$v$	Velocity	$\text{m s}^{-1}$
$\theta$	Angle of detection	Radians
$\alpha$	Animal call/beam width	Radians
$r$	Detection distance	Metres
$p$	Average profile width	Metres
$t$	Time	Seconds
$z$	Number of detections	
$D$	Animal density	animals $\text{m}^{-2}$
$x_i$	Focal Angle $i \in \{1, 2, 3, 4\}$	Radians
$T$	Step length	Seconds
$N$	Number of steps per simulation	
$d$	Time step index	

TABLE 1. List of symbols used to describe the gREM

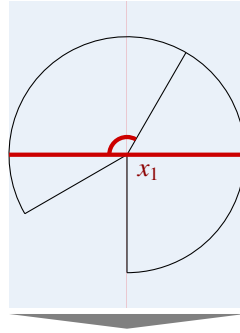


FIGURE 1. The focal angle  $x_1$  used in models with  $\theta > \pi$ . This angle is integrated over to find the average profile size. The sector shaped detection zone (with  $\theta > \pi$ ) is shown in black. The widest part of this region (the profile) is shown with a thick red line and a blue rectangle. The direction of animal movement is downwards, as indicated by the grey arrow.

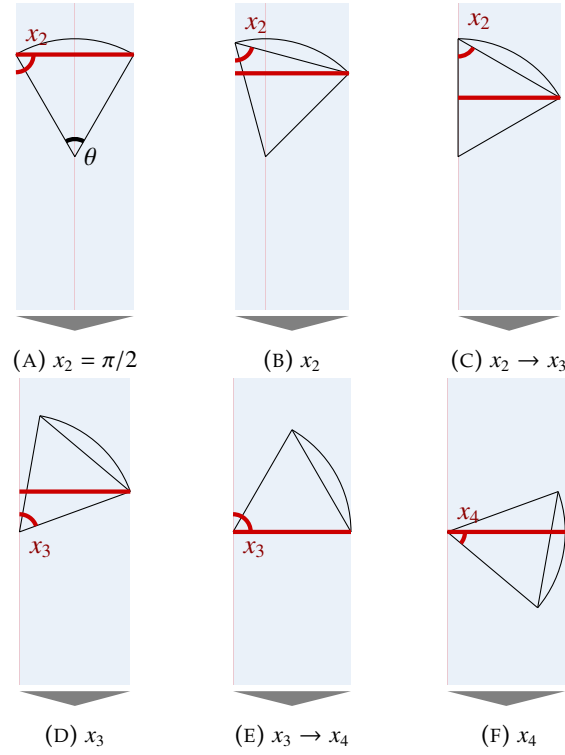


FIGURE 2. The location of the focal angles  $x_{i \in [2,4]}$  and the transitions between them as used in models with  $\theta < \pi$ . These are the angles that are integrated over to find the average profile size. In these figures, the sector shaped detection region is shown in black. The widest part of this region (the profile) is shown with a thick red line and a blue rectangle. The direction of animal movement is always downwards, as indicated by the grey arrow.

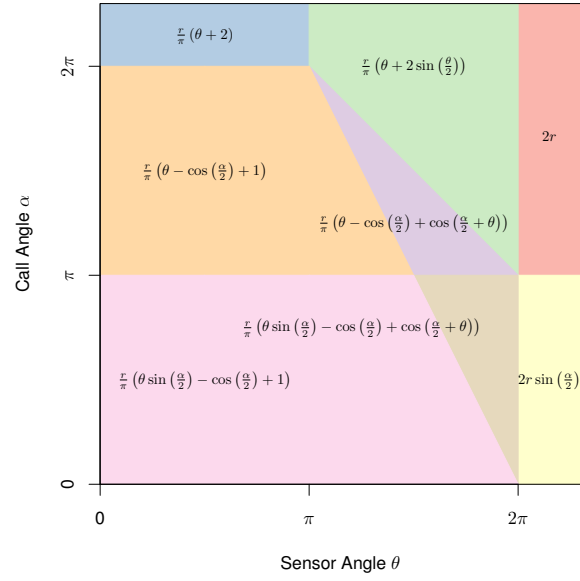


FIGURE 3. Equations for the profile wide,  $p$ , given sensor and call widths. Each colour block represents one equation, despite independent derivation within each block, many models result in the same expression. These are collected together and presented as one block of colour.

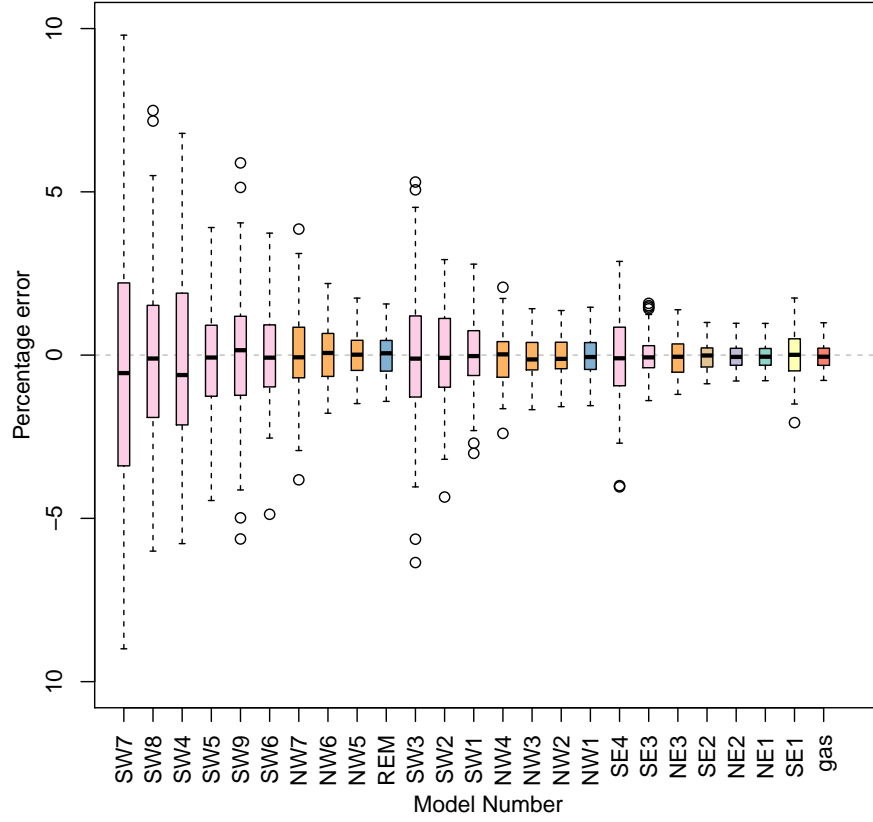


FIGURE 4. Distribution of the bias for each of the derived models. Percentage error of analytical model calculated from the simulation when settings are:  $r = 100$  m;  $T = 150$  days;  $v = 40$  km days<sup>-1</sup>;  $D = 70$  animals km<sup>-2</sup>; and with detection angles varying between models. The number numbers referred to here can be found in Figure 1 Appendix S1, and the colour of each box plot match the functional form of the equation as seen in Figure 3.

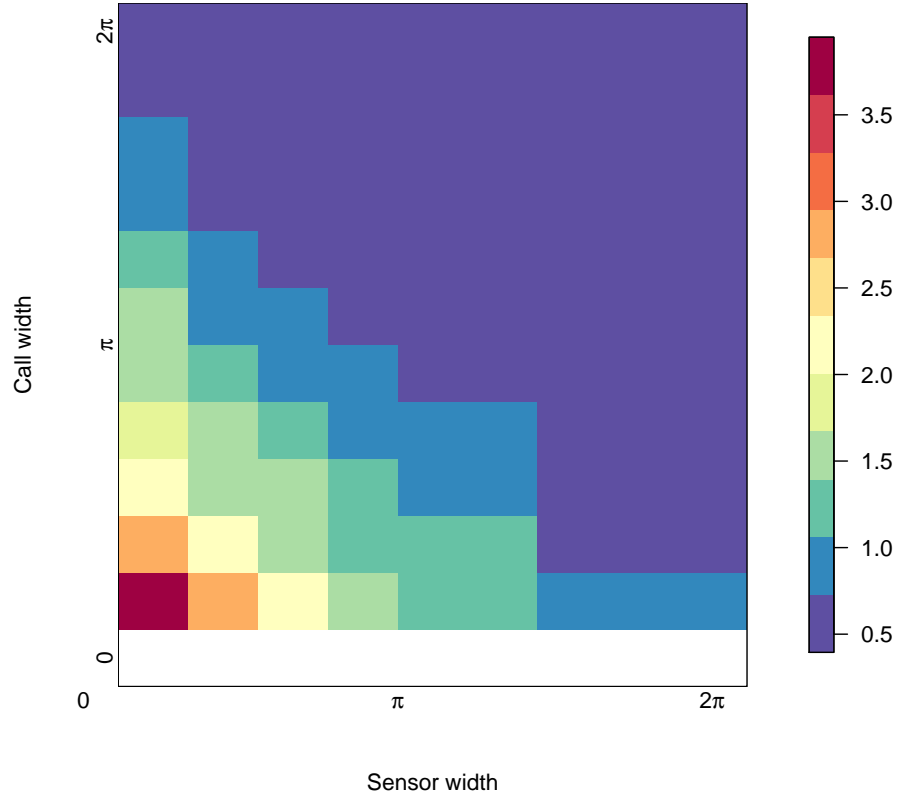


FIGURE 5. Angle of detector

FIGURE 6. The precision of the gREM given a range of detection and call angles. The standard deviation of the percentage error for sensor, and call angles between 0 and  $2\pi$  where:  $r = 100$  m;  $T = 150$  days;  $v = 40$  km days<sup>-1</sup>;  $D = 70$  animals km<sup>-2</sup>; and with detection angles varying between models. Where red indicates a high standard deviation and blue represents a low standard deviation.

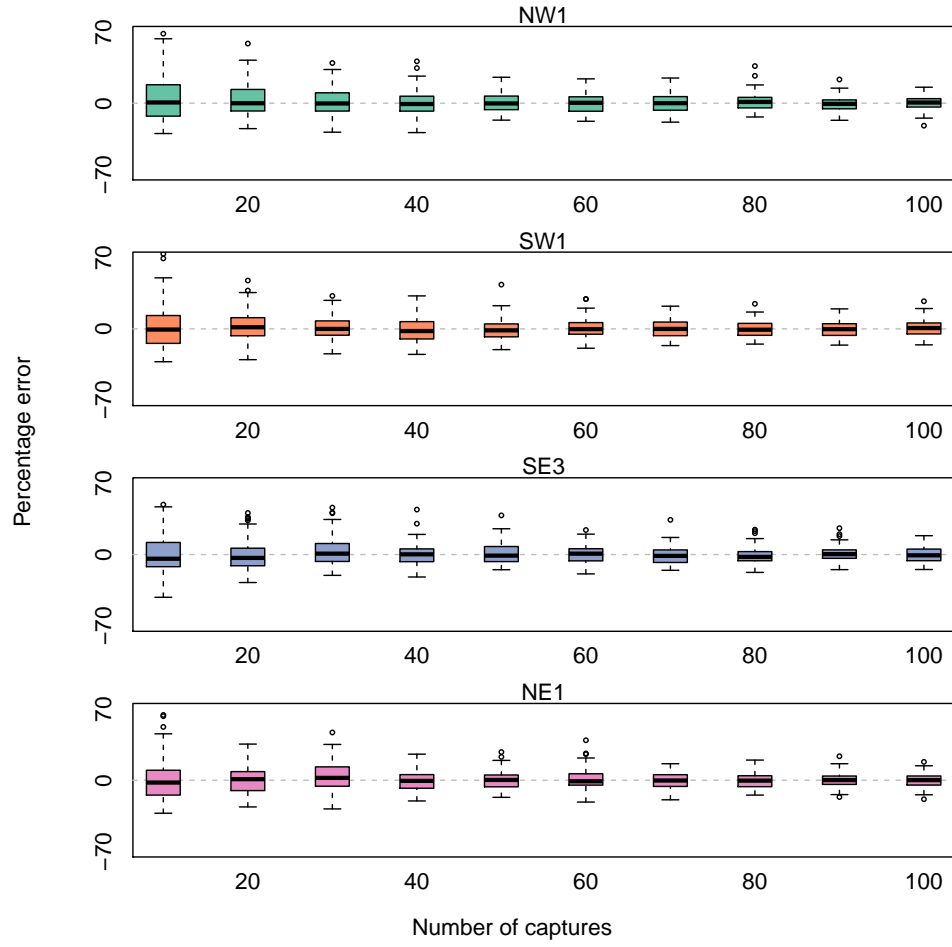


FIGURE 7. Number of captures

FIGURE 8. Accuracy of the gREM reminds unchanged, whilst precision increases, with captures. Boxplots of four test models when given different numbers of captures where:  $r = 100$  m;  $T = 150$  days;  $v = 40$  km days<sup>-1</sup>;  $D = 70$  animals km<sup>-2</sup>; and with angles varying between models. Where the model names refer to Figure 1 in Appendix S1.



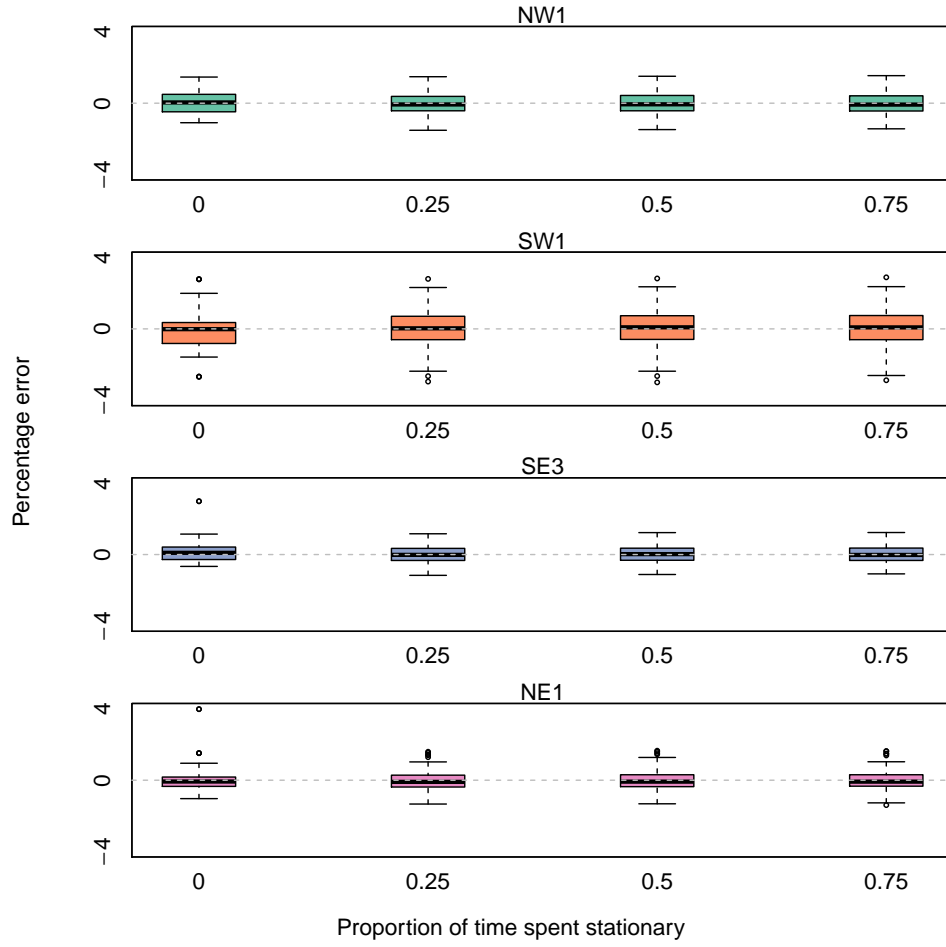


FIGURE 9. Proportion of time spent stationary

FIGURE 10. Accuracy and the precision of the gREM given changes in the amount of time an animal spends stationary on average. Distribution of model error when simulated animals spend increasing proportion of time stationary where:  $r = 100$  m;  $T = 150$  days;  $v = 40$  km days<sup>-1</sup>;  $D = 70$  animals km<sup>-2</sup>; and with detection angles varying between models. Where the model names refer to Figure 1 in Appendix S1.

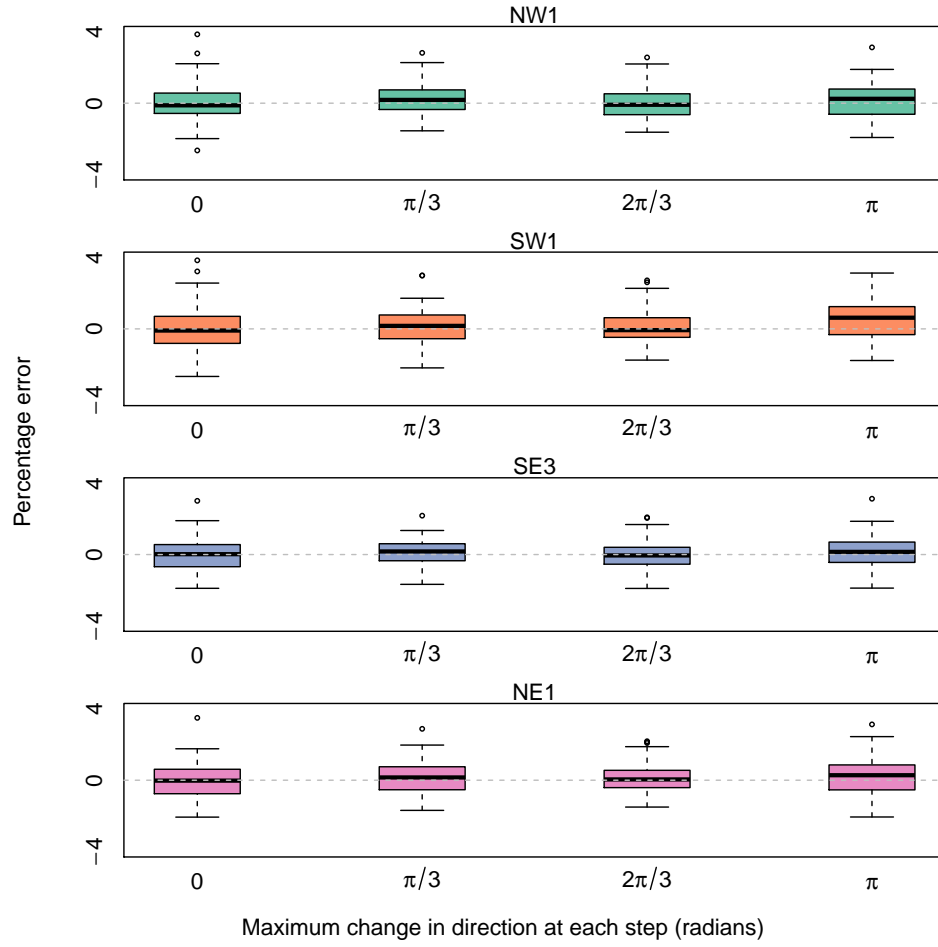


FIGURE 11. Angle of correlated walk

FIGURE 12. Accuracy and the precision of the gREM given different types of correlated walks. Distribution of model error when simulated animals move with different types of correlated walk where:  $r = 10$  m;  $T = 352$  days;  $v = 40$  km days<sup>-1</sup>;  $D = 70$  animals km<sup>-2</sup>; and with angles varying between models. Where the model names refer to Figure 1 in Appendix S1.